Electronic Supplementary Material (ESI) for Nanoscale.

Supplementary Material for

High Potassium Ion Storage Capacity with Long Cycling Stability Enables by Sustainable Oxygen-Rich Carbon Nanosheets

Xuechun Li, Huanlei Wang*, Wenzhe Zhang, Wenrui Wei, Ranxia Liao, Jing Shi, Minghua Huang, Shuai Liu*, Zhicheng Shi

School of Materials Science and Engineering, Ocean University of China, Qingdao 266100, China.

*Corresponding author.

E-mail address: huanleiwang@gmail.com; liushuai6980@ouc.edu.cn

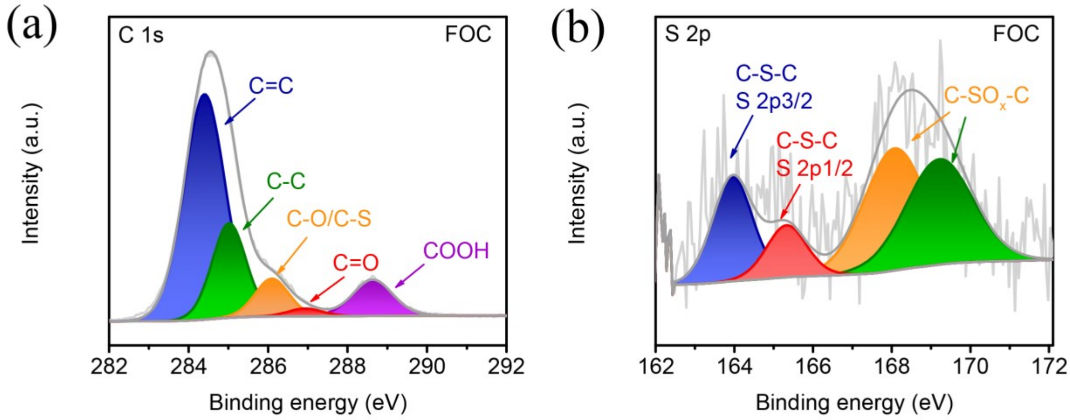

Fig. S1 XPS (a) C 1s spectrum and (b) S 2p spectrum for FOC.

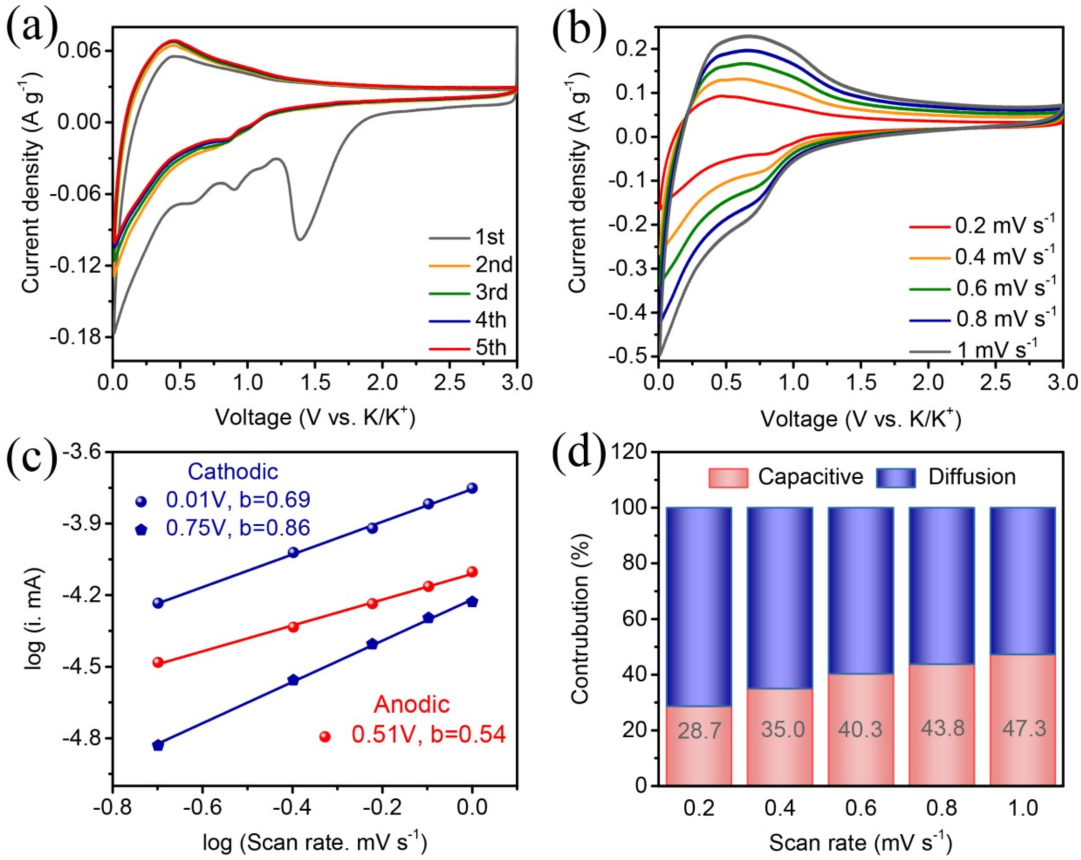

Fig. S2 (a) CV curves of FOC at 0.1 mV s^{-1}. (b) CV curves of FOC at different scan rates from 0.2 to 1 mV s^{-1}. (c) log(*i*) response plotted vs. log(*v*) of FOC at peak voltages. (d) Normalized contribution ratios of capacitive- and diffusion-controlled processes for FOC.

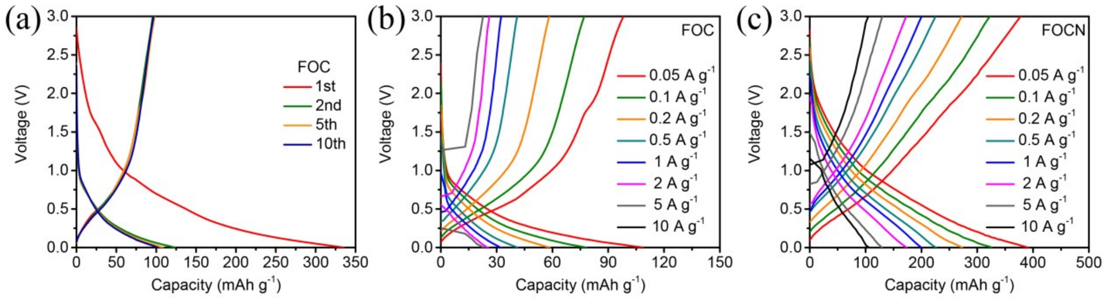

Fig. S3 (a) Galvanostatic charge-discharge curves of FOC at 0.05 A g^{-1} and (b) at different current densities. (c) Galvanostatic charge-discharge curves of FOCN at different current densities.

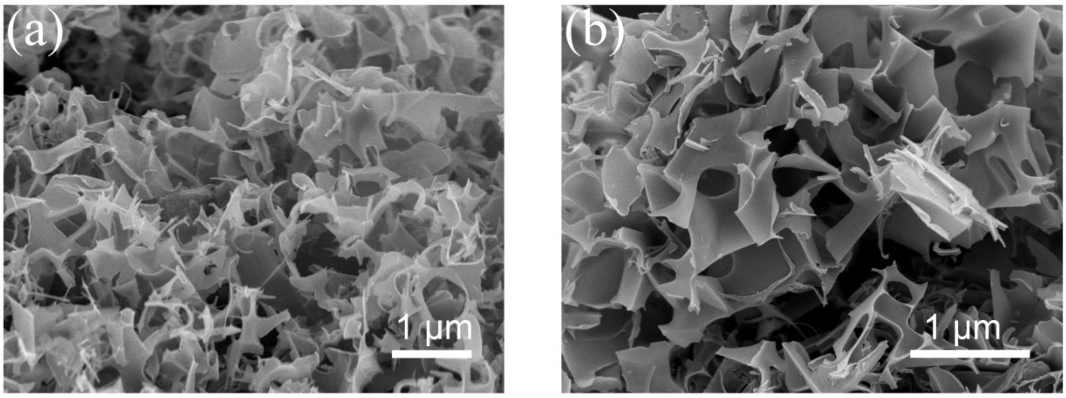

Fig. S4 (a) SEM image of FOCN-5. (b) SEM image of FOCN-15.

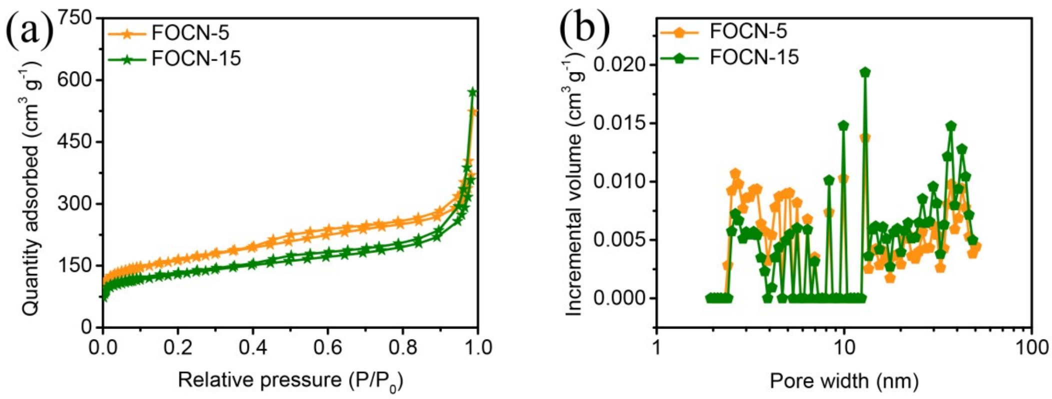

Fig. S5 (a) Nitrogen adsorption-desorption isotherms, and (b) the corresponding pore size distributions of FOCN-5 and FOCN-15.

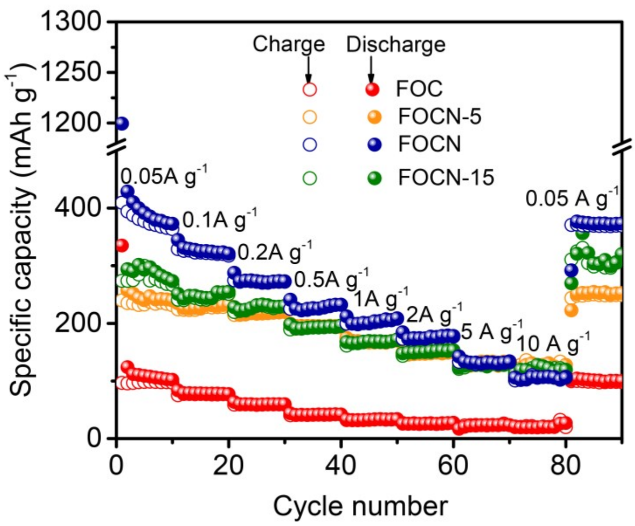

Fig. S6 Rate capability of FOC, FOCN, FOCN-5 and FOCN-15 at current densities from 0.05 to 10 A g^{-1}.

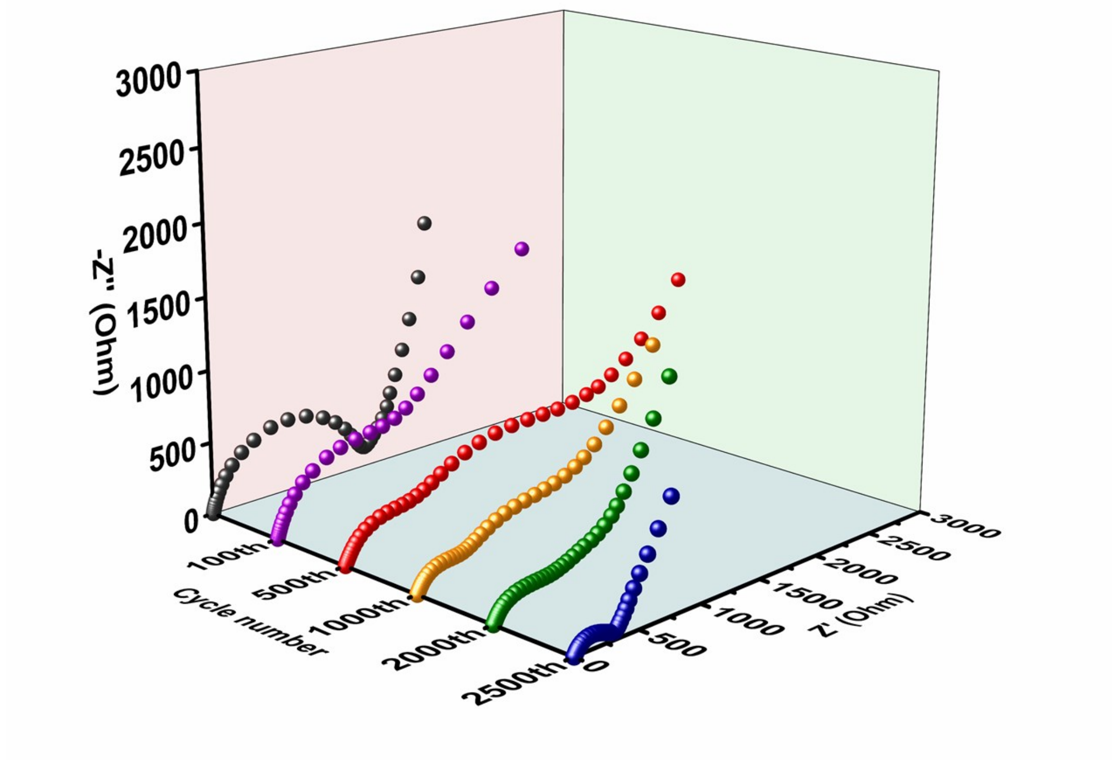

Fig. S7 Nyquist plots of the FOC sample at different cycles at 2 A g^{-1}.

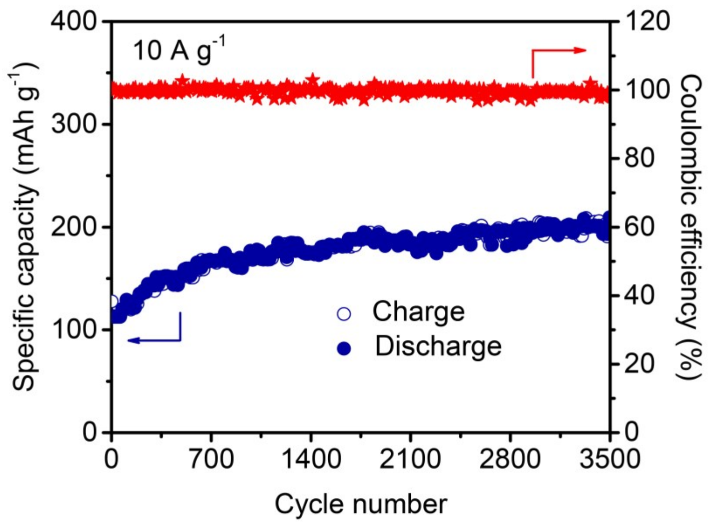

Fig. S8 Long-term cycle performance and the corresponding Coulombic efficiency of the FOCN anode at 10 A g^{-1}.

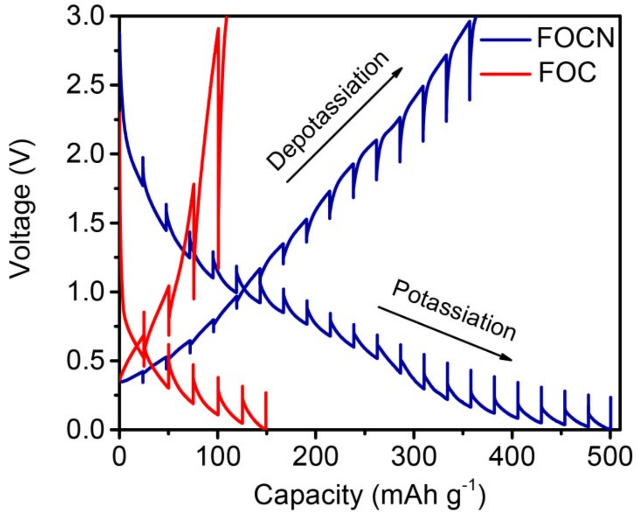

Fig. S9 GITT potential profiles for FOC and FOCN.

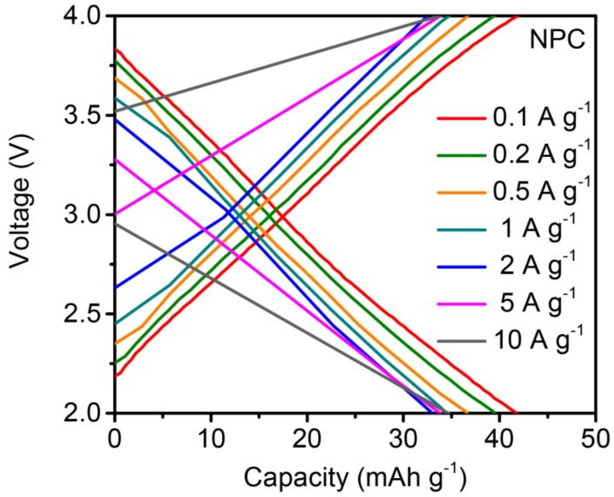

Fig. S10 Galvanostatic charge-discharge profiles for NPC at different current densities (at cycle 5).

(NPC was synthesized by one-step carbonization/activation techniques using methyl cellulose as the precursor, sodium bicarbonate as salt template, urea as N-doping precursor, and potassium hydroxide as activating agent.[1])

Table S1. Physical parameters for FOC and FOCN.

Sample	$d_{(002)}$ (nm)	L_a (nm)	L_c (nm)	I_D/I_G	S_{BET}[a] ($m^2\ g^{-1}$)	S_{mic} ($m^2\ g^{-1}$)	Pore volume[b] (%)		XPS composition (wt%)		
							$V_{<2\ nm}$	$V_{2\text{-}50\ nm}$	C	O	S
FOC	0.376	7.37	1.56	1.70	661	382	86.98	13.02	82.39	17.18	0.42
FOCN	0.379	6.58	1.44	1.90	558	119	18.98	81.02	88.55	9.86	1.59

[a] Surface area was calculated with BET method.

[b] The pore volume was determined by DFT method.

Table S2. Binding energy and relative peak areas of C species evaluated by XPS.

Sample	Peak position (eV)					Relative peak areas (%)				
	C=C	C-C	C-O/C-S	C=O	COOH	C=C	C-C	C-O/C-S	C=O	COOH
FOCN	284.4	285.1	285.9	286.9	289.2	47.91	30.79	7.93	5.09	8.27
FOC	284.4	285.0	286.1	286.9	288.6	59.72	20.98	8.29	1.68	9.34

Table S3. Binding energy and relative peak areas of O species evaluated by XPS.

Sample	Peak position (eV)			Relative content (%)		
	O-S	C=O	C-O-C/C-OH	O-S	C=O	C-O-C/C-OH
FOCN	531.3	532.5	533.9	6.55	47.24	46.20
FOC	531.3	532.4	533.8	5.69	42.92	51.39

Table S4. Binding energy and relative peak areas of S species evaluated by XPS.

Sample	Peak position (eV)				Relative content (%)			
	S $2p_{3/2}$	S $2p_{1/2}$	C-SO_x-C		S $2p_{3/2}$	S $2p_{1/2}$	C-SO_x-C	
FOCN	164.0	165.2	168.3	169.5	44.13	22.70	19.23	13.94
FOC	164.0	165.3	168.1	169.2	20.14	10.05	35.86	33.95

Table S5. Comparison of potassium storage performance between FOCN and other reported carbonaceous electrodes.

Materials	Rate capacity	Cycling performance			Reference
		Current density ($A\ g^{-1}$)	Cycle number	Specific capacity ($mAh\ g^{-1}$)	
FOCN	**392 $mAh\ g^{-1}$ at 0.05 $A\ g^{-1}$ 107 $mAh\ g^{-1}$ at 10 $A\ g^{-1}$**	**2**	**2500**	**301**	**This work**
Sulfur/selenium/nitrogen co-doped hard carbon (SSHC)	252.5 $mAh\ g^{-1}$ at 0.1 $A\ g^{-1}$ 158.1 $mAh\ g^{-1}$ at 3 $A\ g^{-1}$	1	1100	143.5	2
N/O co-doped porous hard carbon nanobelts (NOCNBs)	468 $mAh\ g^{-1}$ at 0.05 $A\ g^{-1}$ 200 $mAh\ g^{-1}$ at 3.2 $A\ g^{-1}$	1	1600	277	3
N/P co-doped vertical graphene on CC (N, P-VG@CC)	335.6 $mAh\ g^{-1}$ at 0.025 $A\ g^{-1}$ 156.1 $mAh\ g^{-1}$ at 2 $A\ g^{-1}$	1	1000	142.4	4
Carbon dots@rGO (CDs@rGO)	309 $mAh\ g^{-1}$ at 0.1 $A\ g^{-1}$ 221 $mAh\ g^{-1}$ at 0.5 $A\ g^{-1}$	0.2	840	244	5
Edge-enriched N-doped porous carbon nanosheets (ENPCS)	276 $mAh\ g^{-1}$ at 0.05 $A\ g^{-1}$ 110 $mAh\ g^{-1}$ at 4 $A\ g^{-1}$	1	6000	252	6
Volcanic-like hard carbon (PNTCDA)	220.7 $mAh\ g^{-1}$ at 0.1 $A\ g^{-1}$ 103 $mAh\ g^{-1}$ at 4 $A\ g^{-1}$	2	4000	81	7
N/S dual-doped carbon (N, S-3DHPC)	380.5 $mAh\ g^{-1}$ at 0.1 $A\ g^{-1}$ 129.4 $mAh\ g^{-1}$ at 10 $A\ g^{-1}$	1	1000	249.5	8
Soybeans-derived hard carbon (SC-500)	175 $mAh\ g^{-1}$ at 0.05 $A\ g^{-1}$ 70 $mAh\ g^{-1}$ at 0.8 $A\ g^{-1}$	0.05	900	196	9

N-doped porous carbon (NHPC)	305.7 mAh g^{-1} at 0.05 A g^{-1} 102.6 mAh g^{-1} at 2 A g^{-1}	1	1000	119.9	10
Oxygen-rich carbon nanosheets (CNSs)	252 mAh g^{-1} at 0.1 A g^{-1} 133 mAh g^{-1} at 10 A g^{-1}	2	1300	147	11
Onion-like carbon (OLC)	179 mAh g^{-1} at 0.1 A g^{-1} 78 mAh g^{-1} at 10 A g^{-1}	2	1000	111	12
3D nitrogen-doped framework carbon (3DNFAC)	309 mAh g^{-1} at 0.1 A g^{-1} 111 mAh g^{-1} at 10 A g^{-1}	2	1000	137	13
Hierarchically porous thin carbon shells (S/N@C)	235 mAh g^{-1} at 0.1 A g^{-1} 64 mAh g^{-1} at 4 A g^{-1}	2	900	65	14
S/O co-doped hard carbon (PCMs)	230 mAh g^{-1} at 0.05 A g^{-1} 158 mAh g^{-1} at 1 A g^{-1}	1	2000	108.4	15

Table S6. Peak areas of O species evaluated by *ex-situ* XPS.

State	Relative content (%)		
	C=O	C-O-C/C-OH/S=O	O-S
Pristine	**47.24**	46.20	6.55
Fully discharged (cycle 1)	**11.17**	82.51	6.31
Fully charged (cycle 1)	**45.04**	48.93	6.03
Fully charged (cycle 2500)	**78.41**	12.74	8.85

Table S7. Peak areas of S species evaluated by *ex-situ* XPS.

State	Relative content (%)					
	S $2p_{3/2}$	S $2p_{1/2}$	S^{2-}	KSO_X	Thiosulfate/sulfate/-SO_2-	
Fully charged (cycle 1)	8.88	4.18	8.30	16.99	45.53	16.11
Fully charged (cycle 2500)	13.17	6.60	8.94	15.12	41.49	14.68

Table S8. Electrochemical performance of FOCN//NPC PIHC devices compared with previously reported PIHCs, SIHCs and LIHCs.

Anode materials	Cathode materials	Electrochemical performance	Reference
FOCN	**NPC**	**193 Wh kg^{-1} at 494 W kg^{-1}** **20 Wh kg^{-1} at 22324 W kg^{-1}**	**This work**
N-rich activated carbon (SEG)	N-rich activated carbon (SEG)	51 Wh kg^{-1} at 600 W kg^{-1} 25 Wh kg^{-1} at 9600 W kg^{-1}	16
Graphite	Activated carbon	57.8 Wh kg^{-1} at 1422 W kg^{-1} 18.8 Wh kg^{-1} at 15887 W kg^{-1}	17
U-Co_2P@rGO-14	Activated carbon	87 Wh kg^{-1} at 12 W kg^{-1} 10 Wh kg^{-1} at 4264.7 W kg^{-1}	18
$Ca_{0.5}Ti_2(PO_4)_3$@C (CTP@C)	Activated carbon	80 Wh kg^{-1} at 32 W kg^{-1} 34 Wh kg^{-1} at 5144 W kg^{-1}	19
$K_2Ti_6O_{13}$ (KTO)	N-doped nanoporous graphenic carbon (NGC)	58.2 Wh kg^{-1} at ~166 W kg^{-1} 13.2 Wh kg^{-1} at 7200 W kg^{-1}	20
Hollow carbon (HC)	Boron-doped graphite (BG)	108 Wh kg^{-1} at 495 W kg^{-1} 20 Wh kg^{-1} at 6100 W kg^{-1}	21
Nb_2O_5@C/rGO-50	MSP-20	76 Wh kg^{-1} at 80 W kg^{-1} 6 Wh kg^{-1} at 20800 W kg^{-1}	22
TiO_2@CNT@C	Biomass-derived activated carbon (BAC)	81.2 Wh kg^{-1} at 126 W kg^{-1} 37.9 Wh kg^{-1} at 12400 W kg^{-1}	23
V_2O_5-CNT	Activated carbon	38 Wh kg^{-1} at 140 W kg^{-1} 7.5 Wh kg^{-1} at 5000 W kg^{-1}	24

MWTOG	Activated carbon	64.2 Wh kg^{-1} at 56.3 W kg^{-1} 25.8 Wh kg^{-1} at 1357 W kg^{-1}	25
Graphene-wrapped $Li_4Ti_5O_{12}$ (LTO)	Activated carbon	50 Wh kg^{-1} at ~18 W kg^{-1} 15 Wh kg^{-1} at 2500 W kg^{-1}	26
TiO_2/CNT	Activated carbon	59.6 Wh kg^{-1} at 120 W kg^{-1} 22.3 Wh kg^{-1} at 13900 W kg^{-1}	27

Supporting References

1. Y. P. Cui , W. Liu, Y. Lyu, Y. Zhang, H. L. Wang, Y. J. Liu and D. Li, *J. Mater. Chem. A*, 2018, **6**, 18276-18285.
2. Y. Liu, H. D. Dai, Y. K. An, L. J. Fu, Q. Y. An and Y. P. Wu, *J. Mater. Chem. A*, 2020, **8**, 14993-15001.
3. K. Zhang, Q. He, F. Y. Xiong, J. P. Zhou, Y. Zhao, L. Q. Mai and L. N. Zhang, *Nano Energy*, 2020, **77**, 105018.
4. W. D. Qiu, H. B. Xiao, Y. Li, X. H. Lu and Y. X. Tong, *Small*, 2019, **15**, 1901285.
5. E. Zhang, X. X. Jia, B. Wang, J. Wang, X. Z. Yu and B. G. Lu, *Adv. Sci.*, 2020, **7**, 2000470.
6. F. Xu, Y. X. Zhai, E. Zhang, Q. H. Liu, G. S. Jiang, X. S. Xu, Y. Q. Qiu, X. M. Liu, H. Q. Wang and S. Kaskel, *Angew. Chem. Int. Ed.*, 2020, **59**, 2-10.
7. Y. Liu, Q. Ru, Y. Q. Gao, Q. Y. An, F. M. Chen, Z. L. Shi, M. H. Zheng and Z. K. Pan, *Appl. Surf. Sci.*, 2020, **525**, 146563.
8. B. B. Fan, J. X. Yan, A. P. Hu, Z. Liu, W. Z. Li, Y. H. Li, Y. L. Xu, Y. Zhang, Q. L. Tang, X. H. Chen and J. L. Liu, *Carbon*, 2020, **164**, 1-11.
9. L. Tao, L. Liu, R. F. Chang, H. B. He, P. Zhao and J. Liu, *J. Power Sources*, 2020, **463**, 228172.
10. C. L. Gao, Q. Wang, S. H. Luo, Z. Y. Wang, Y. H. Zhang, Y. G. Liu, A. M. Hao and R. Guo, *J. Power Sources*, 2019, **415**, 165-171.
11. J. T. Chen, B. J. Yang, H. J. Hou, H. X. Li, L. Liu, L. Zhang and X. B. Yan, *Adv. Energy Mater.*, 2019, **9**, 1803894.
12. J. T. Chen, B. J. Yang, H. X. Li, P. J. Ma, J. W. Lang and X. B. Yan, *J. Mater. Chem. A*, 2019, **7**, 9247-9252.
13. B. J. Yang, J. T. Chen, L. Y. Liu, P. J. Ma, B. Liu, J. W. Lang, Y. Tang and X. B. Yan, *Energy Storage Mater.*, 2019, **23**, 522-529.
14. A. Mahmood, S. Li, Z. Ali, H. Tabassum, B. J. Zhu, Z. B. Liang, W. Meng, W. Aftab, W. H. Guo, H. Zhang, M. Yousaf, S. Gao, R. Q. Zou and Y. S. Zhao, *Adv. Mater.*, 2019, **31**, 1805430.

15. M. Chen, W. Wang, X. Liang, S. Gong, J. Liu, Q. Wang, S. J. Guo and H. Yang, *Adv. Energy Mater.*, 2018, **8**, 1800171.
16. Z. Chen, W. L. Li, J. Yang, J. X. Liao, C. Chen, Y. C. Song, S. A. Ali Shah, Z. Q. Xu and M. Q. Wu, *J. Electrochem. Soc.*, 2020, **167**, 050506.
17. X. Liu, G. A. Elia, B. S. Qin, H. Zhang, P. Ruschhaupt, S. Fang, A. Varzi and S. Passerini, *ACS Energy Lett.*, 2019, **4**, 2675-2682.
18. Y. X. Wang, Z. Y. Zhang, G. X. Wang, X. Y. Yang, Y. M. Sui, F. Du and B. Zou, *Nanoscale Horiz.*, 2019, **4**, 1394-1401.
19. Z. Y. Zhang, M. L. Li, Y. Gao, Z. X. Wei, M. N. Zhang, C. Z. Wang, Y. Zeng, B. Zou, G. Chen and F. Du, *Adv. Funct. Mater.*, 2018, **28**, 1802684.
20. S. Dong, Z. Li, Z. Xing, X. Wu, X. Ji and X. Zhang, *ACS Appl. Mater. Interfaces*, 2018, **10**, 15542-15547.
21. F. Yu, Z. C. Liu, R. W. Zhou, D. M. Tan, H. X. Wang and F. X. Wang, *Mater. Horiz.*, 2018, **5**, 529-535.
22. E. Lim, C. Jo, M. S. Kim, M.-H. Kim, J. Chun, H. Kim, J. Park, K. C. Roh, K. Kang, S. Yoon and J. Lee, *Adv. Funct. Mater.*, 2016, **26**, 3711-3719.
23. Y.-E. Zhu, L. P. Yang, J. Sheng, Y. N. Chen, H. C. Gu, J. P. Wei and Z. Zhou, *Adv. Energy Mater.*, 2017, **7**, 1701222.
24. Z. Chen, V. Augustyn, X. L. Jia, Q. F. Xiao, B. Dunn and Y. F. Lu, *ACS Nano*, 2012, **6**, 4319-4327.
25. Z. Le, F. Liu, P. Nie, X. Li, X. Liu, Z. Bian, G. Chen, H. B. Wu and Y. Lu, *ACS Nano*, 2017, **11**, 2952-2960.
26. H. Kim, K.-Y. Park, M.-Y. Cho, M.-H. Kim, J. Hong, S.-K. Jung, K. C. Roh and K. Kang, *ChemElectroChem*, 2014, **1**, 125-130.
27. Z. Chen, Y. Yuan, H. Zhou, X. Wang, Z. Gan, F. Wang and Y. Lu, *Adv. Mater.*, 2014, **26**, 339-345.